Physica C 192 (1992) 284–292
North-Holland

PHYSICA C

Unconventional superconductivity in UPt_3 low field AC susceptibility studies

Z. Kozioł, J.J.M. Franse, P. de Châtel, T. Vorenkamp, K. Bakker, A. de Visser and A.A. Menovsky

Van der Waals–Zeeman Laboratorium der Universiteit van Amsterdam, Valckenierstraat 65, 1018 XE Amsterdam, Netherlands

Received 1 November 1991

Low-field AC susceptibility measurements have been carried-out on single-crystalline samples of the unconventional superconductor UPt_3 and on UPt_3 doped with 11% boron. Both components of the susceptibility, $\chi'(T)$ and $\chi''(T)$ have been found to depend strongly on the AC field amplitude, on the superimposed DC field (up to 200 Oe), and on the orientation of the field with respect to crystallographic axes. A discussion of the experimentally determined penetration depth close to T_c is presented, leading to the conclusion that the mechanism described by Campbell makes a large contribution to the field penetration into the superconductor. A phase diagram constructed on the basis of field penetration into the bulk sample is only partly in agreement with $H_{c1}(T)$ results published earlier. We argue that a vortex-glass state may be formed in UPt_3 close to T_c, due to the coupling between the AF and unconventional SC order parameters.

1. Introduction

The unconventional nature of the superconducting order parameter in UPt_3 seems to be well documented. The microscopic origin and the symmetry class, however, are still not clear [1]. The anisotropic properties of the superconducting state close to T_c have been revealed in a number of experiments: ultrasound attenuation [2,3], thermal expansion [4,5], radio-frequency susceptibility [6] and thermal conductivity [7]. Significant anisotropies have been reported for the first [8] and second critical field [9,10]. The splitting of the superconducting transition observed as a two-step anomaly in the specific heat [11] and as a change in the slope of H_{c1} and of H_{c2} is possibly due to the interaction between the superconducting (SC) and antiferromagnetic (AF) order parameters [12–14].

However, some discrepancy between the different results reported for the electrodynamic properties can be noticed. The $H_{c1}(T)$ values are not consistent between different reports (see table 1). There are differences in the position of the kink temperature and in the slope dH_{c1}/dT. There is no consistency between H_{c1} and reported values of λ, the penetration depth, at low temperatures, if the usual relation between them is used: $H_{c1} = \phi_0 \ln \kappa_{GL}/4\pi\lambda^2$, where κ_{GL} is the Ginzburg–Landau parameter. Furthermore, the low temperature behaviour seems to depend on the experimental method: at $T \ll T_c$, $\lambda(T) - \lambda(0) \sim T^{\nu}$ is obtained with ν close to 2 in DC measurements [15] whereas $\nu \approx 4$ is deduced from the high-frequency susceptibility [16]. This disagreement between $\lambda(T)$ obtained in different ways is believed to be caused by the frequency dependence of the penetration depth [17], a property connected with the nodal structure

Table 1
Summary of the reported results for H_{c1} (after analysis of the results contained in the cited references)

$T_c^+ - T_{kink}$	$-dH_{c1}/dT$ (Oe/10 mK)		Ref.
	$H \parallel c$	$H \parallel a, b$	
180	–	2	[8]
75	5.6	4.3	[9]
no kink	–	1.2	[19]
50	4.0	4.1	[22]
63	–	2	[26]
145	2.7	2.1	[40]

of the gap function. Magnetic relaxation effects have been observed in the superconducting state at fields comparable to H_{c1} [18,19]. This observation focuses the attention on the possibility that dynamic effects, together with the finite value of the supercurrent induced in the material during $M(H)$ measurements, disturbs the determination of the first critical field. A similar situation has been found in high-T_c superconductors [20].

The most realistic values of H_{c1} are obtained from the London penetration depth deduced from μ^+-spin relaxation measurements of the distribution of internal fields in the mixed state [21]. This method yields $\lambda(0) \approx 0.8\mu m$, which implies $H_{c1}(0) = 13$ Oe, a value 5–10 times smaller than the results of other measurements. It should be noted, however, that in order to deduce λ from μ^+-relaxation data the conventional vortex core structure must be assumed.

The height of the specific heat jump at T_c can be used to determine the thermodynamic critical field. $H_c(0)$ obtained in this way (about 250 Oe) is close to reported values of $H_{c1}(0)$ [22], contrary to the expectations based on the large Ginzburg–Landau parameter κ_{GL}.

In this paper we present the results of a systematic study of the electrodynamic properties of pure and boron-doped UPt_3 in the SC state by means of AC-susceptibility measurements, extending investigations of Piquemal et al. [23]. Measurements of the AC susceptibility have been carried out on rather pure single-crystalline samples, characterised in table 2. As the superconducting properties of UPt_3 are known to depend strongly on sample preparation, it is important to have a wide class of results obtained on physically identical samples. Some preliminary measurements of the AC susceptibility on two of the samples investigated here (samples A and B in table 2) have been published [24], together with the specific heat and resistivity results. For samples C and D the field dependence of the two-step anomaly in $C(T)$ and H_{c2} measured resistively have been described [25]. The first critical field for samples C and D has been investigated by $M(H)$ measurements [26]. In the present work an unexpected, large difference is reported in the AC susceptibility measured with the AC field parallel and perpendicular to the c-axis. The AC susceptibility is found to be independent of amplitude at lower temperatures up to rather high values of the AC field. This is manifested in the lack of temperature dependence in χ'' below a certain temperature, which however does depend on the AC field amplitude. In this temperature region the value of χ'' is very close to zero. The observed $\lambda(T)$ dependence implies that the sample is not in the pure Meissner state. The results are consistent with the temperature dependence of Campbell's penetration depth [27], which is supposed to be relevant in the presence of an interaction of the current with pinned vortices [28]. That interaction gives a contribution to the reactive part of the complex impedance, increasing strongly the observed penetration depth above the London penetration depth. The paper is organised as follows. In section 2 the samples are characterised and the experimental details are described. The basic experimental results are contained in section 3 with their detailed analysis in section 4. An explanation of the observed temperature dependence of the penetration depth is proposed, based on the notion of a glassy state in UPt_3 due to the coupling between the antiferro-

Table 2
Sample characterisation

Sample	size $a \times b \times c$ (mm^3)	ρ_0 ($\mu\Omega$ cm)	A ($\mu\Omega$ cm/K^2)	T_c (mK) at $\rho = 0$	
UPt_3					
A	$0.6 \times 0.65 \times 3.6$	0.70	0.69	446	$H \parallel c$
B	$0.9 \times 8 \times 1.15$	1.35	1.65	443	$H \parallel b$
UPt_3+11%B					
C	$3.0 \times 0.3 \times 4.0$	0.27	0.82	548	$H \parallel c$
D	$0.87 \times 5.0 \times 0.88$	0.45	1.75	545	$H \parallel b$

agnetic and superconducting order parameters, as put forward by Joynt et al. [29].

2. Samples and details of measurements

Samples were prepared by the Czochralski method [30]. A suitable, rectangular shape has been realised by spark erosion. Results are reported for two pairs of samples, each pair originating from the same batch: sample A and B are pure UPt_3 materials, while samples C and D are of UPt_3 doped with 11% boron (nominal concentration). The boron doped samples have been found [25] to possess exceptional superconducting properties: relatively high T_c with a well pronounced double SC transition observed in specific heat measurements. The largest dimension for samples A and C is along the crystallographic c direction and for samples B and D along the b direction. In the susceptibility measurements the field was applied for samples A and C along the c-axis, and for B and D along the b direction. The onset temperature of the superconducting transition in $C(T)$ is the same for samples A and B and the same for C and D. For each sample a trace of the two-step transition can be noticed. For the resistivity the temperature dependence $\rho=\rho_0+AT^2$, typical for heavy-fermion systems, is observed at low temperatures, with ρ_0 and A given in table 2. The AC susceptibiiity has been measured by a mutual inductance method using a PAR 5208 lock-in amplifier in a computer-controlled system. Both components of the susceptibility, χ' and χ'' were registered simultaneously. In the data analysis we assume that the sample geometry can be approximated by the shape of a long cylinder. In the superconducting state, the two-fluid model is used to describe the magnetic field distribution in the sample. Using the Maxwell equations, one obtains the following result for the field penetration into the material filling the half-space $x>0$:

$$B=B_0\,\eta(x)\exp(i\omega t)\,. \tag{1}$$

A differential equation is obtained for the function $\eta(x)$, the solution being

$$\eta(x)=\exp(-x\kappa)\,, \tag{2}$$

where the κ is given in terms of the normal state skin depth δ and of the penetration depth λ connected with the imaginary part of the complex conductivity in the superconducting state:

$$\kappa^2=-1/\lambda^2+2i/\delta^2\,, \tag{3}$$

$$\delta^2=\frac{C^2}{2\pi\omega\sigma}\,, \tag{4}$$

where σ is the normal state conductivity and $\omega=2\pi f$ is the circular frequency of the applied AC field. With these parameters, the complex AC susceptibility of a long cylinder of radius d is written [31] as

$$4\pi\chi=-1+(2/\kappa d)J_1(\kappa d)/J_0(\kappa d)\,, \tag{5}$$

where J_ν are the Bessel functions given by the infinite series:

$$J_\nu(z)=(z/2)^\nu\sum_{n=0}^{\infty}(-1/4z^2)^n/n!(n+\nu)!\,. \tag{6}$$

For the field applied along the axis of the cylinder the demagnetisation coefficient D is equal to 0. For the samples used by us D is also small, close to 0.2. We normalise the low temperature susceptibility to $-1/4\pi$. The difference between the actual susceptibility and the measured one, due to the finite demagnetisation effect, is negligible, as long as $4\pi\chi'+1\ll 1$. The error introduced by the procedure is only significant close to T_c, when $|\chi|\ll 1/4\pi$. However, close to T_c the sample is no longer in the Meissner state, as we will show, even for small AC field: a large χ'', dependent on the amplitude of the AC field, is observed. Then any correction for the demagnetisation effect is bound to be inaccurate, as the detailed current distribution in the sample is unknown. Summarizing: we normalise the low-T part of $\chi'(T)$ to a value close to $-1/4\pi$ and the error introduced in this way has little influence on the analysis.

Most of the results were obtained with an AC frequency of 1000 Hz. At this frequency the normal-state skin depth is still a few times larger than the sample dimension and then both components of the susceptibility in the normal state are very small. Although we observe some frequency dependence of χ, essentially the same results are obtained at much lower frequencies.

3. Complex susceptibility of UPt_3

The temperature dependence of the complex susceptibility of the pure UPt_3 samples is shown in fig. 1, for AC field parallel (sample A) and orthogonal (sample B) to the c-axis. Large differences are observed between these two orientations. The onset of diamagnetism is observed in χ' at a temperature about 30 mK lower for the AC field along the c direction. A strong AC field dependence is observed in relatively low field. The $d\chi'/dT$ extrema correspond well to the maxima in $\chi''(T)$. For the c-axis sample the two-step transition is clearly observed both, in $\chi'(T)$ and in $\chi''(T)$. At low AC fields, the maximum values of $\chi''(T)$ are much smaller than what is expected in the critical state (about $0.2/4\pi$, [32]), where the losses are connected with the hysteretic magnetic response of a superconductor. Such a situation can be expected for the AC field amplitude exceeding the first critical field. For higher fields, the maximum tends to be close to about $0.4/4\pi$, the flux-flow result [33]. A similar conclusion follows from the results on the boron-doped samples (fig. 2). However, the double-step structure in $\chi(T)$ is not observed here. One can observe that below a certain temperature, which depends on the amplitude of the AC field, the imaginary part becomes temperature independent and is equal to zero within the accuracy of our measurements. We have checked that for a given AC-field amplitude this temperature is independent of the frequency of the applied field, with an accuracy of about 5 mK, within about two decades of the frequency.

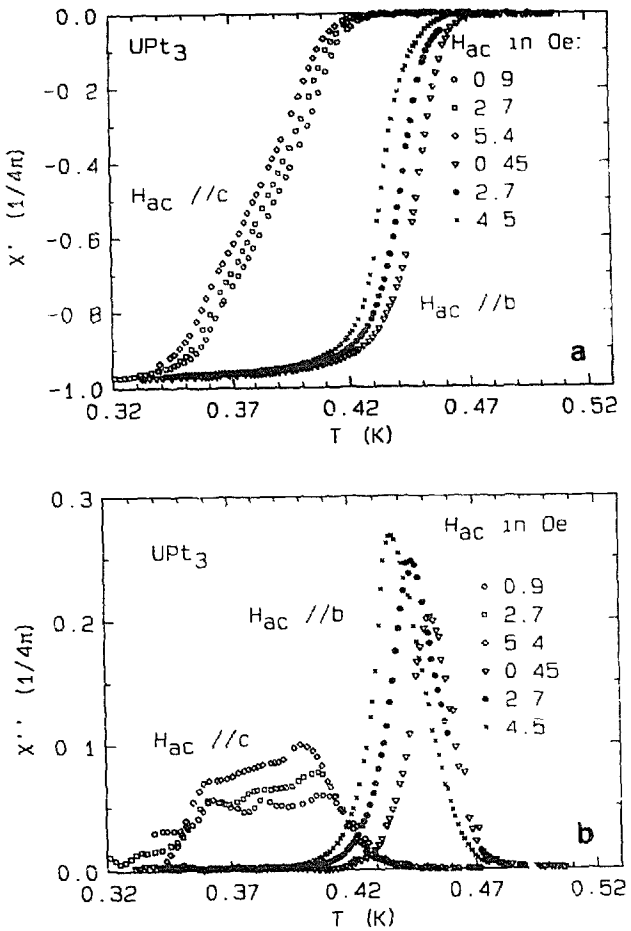

Fig. 1. (a) the real part χ', and (b) the imaginary part χ'' of the complex AC susceptibility of UPt_3 single crystalline samples.

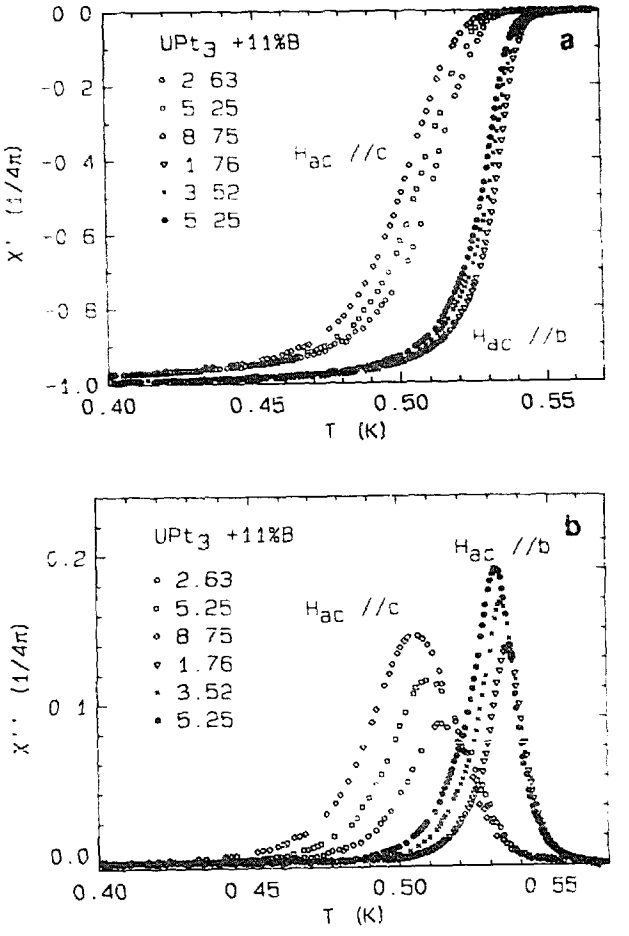

Fig. 2. (a) the real part χ', and (b) the imaginary part χ'' of the complex AC susceptibility of UPt_3 doped with 11% boron for a set of AC field amplitudes.

Figure 3 presents the results on the influence of a DC field on the AC susceptibility measured with a low AC amplitude. The DC field is causing a much smaller shift of the curves toward lower temperatures than an AC field of similar value. This observation implies that a finite value of the critical current, which is field dependent, is responsible for the field dependence of the AC susceptibility, rather than the effects connected with the crossing of the critical fields, for instance of H_{c1}, during a temperature sweep. A similar conclusion follows from the results of fig. 4. There, for several stabilised temperatures, the changes of χ' and χ'' measured at low AC field (0.2 Oe) are shown after applying a DC field (in zero-field-cooled samples). χ' is strongly dependent on the DC field, already at low fields. This is not a good method to determine H_{c1}; we do not observe any change in the character of $\chi'(H_{DC})$ at the DC field value close to H_{c1} expected on the basis of $M(H)$ measurements [26]. There is a difference between our $\chi'(H_{DC})$ and that of Shivaram et al. [8], where a very similar method, albeit with higher frequency and smaller AC field, was used successfully to clearly determine H_{c1}. Although χ' is observed to depend on H_{DC} at any finite field and at any temperature, χ'' shows a different behaviour, being independent of the DC field, with high accuracy, if the field or temperature are not too high (see data for $T=475$ mK in fig. 4(b)).

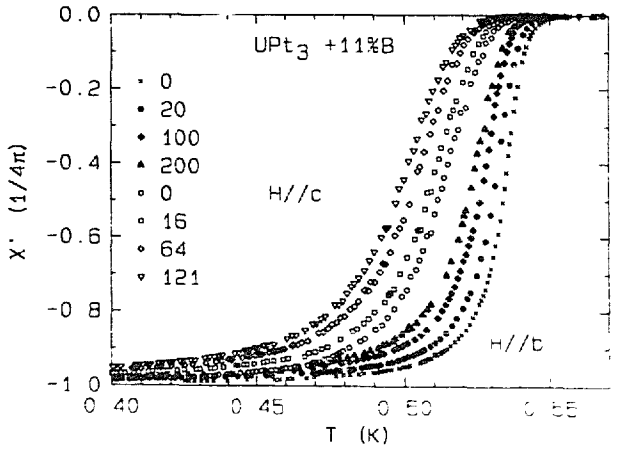

Fig. 3. The influence of a DC field on the real part of the AC susceptibility of samples doped with boron, measured in an AC field of 1 kHz and 0.35 Oe in amplitude on field-cooled samples. DC field values (in Oe) are given in the figure.

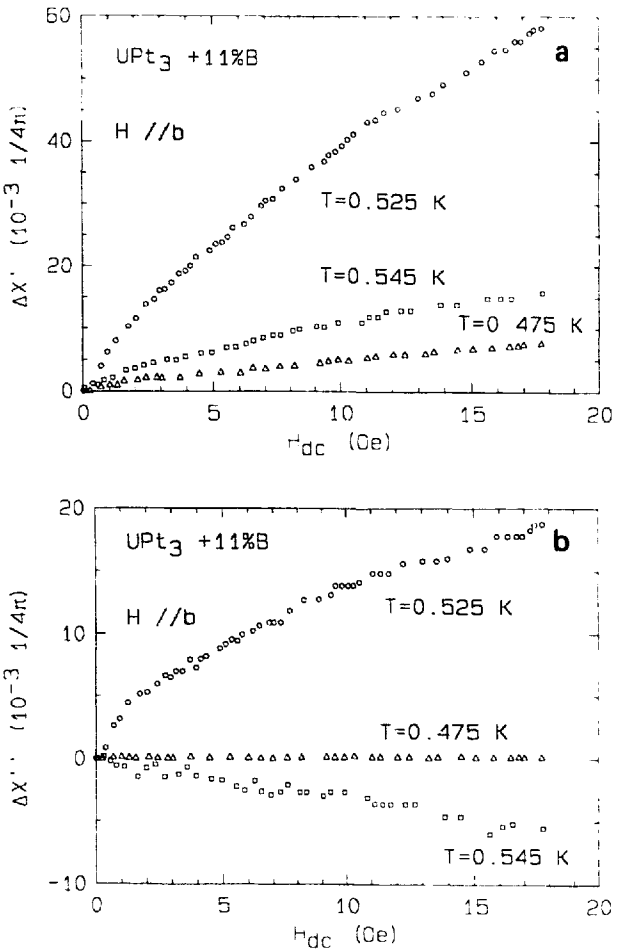

Fig. 4. Field dependence of χ' (a) and of χ'' (b), measured on sample D in the zero-field-cooled states at stable temperatures. The changes of the susceptibility in comparison with $\chi(H_{DC}=0)$ are presented.

4. Analysis of the results

The following picture emerges after an analysis of the above results. At high enough AC field, the current density induced in the sample approaches the critical current density j_c. At small AC field the response resembles the Meissner-state behaviour. However, a DC field has an influence on χ_{AC}, which is different from the response expected in the Meissner state. In particular χ should not be amplitude dependent and χ'' should vanish in a proper Meissner state. The strong amplitude dependence of the AC susceptibility is illustrated in fig. 5, representing plots of χ'' versus χ' for different amplitudes. There is a tendency toward the flux-flow dependence, for higher AC fields. The solid line in the figure has been

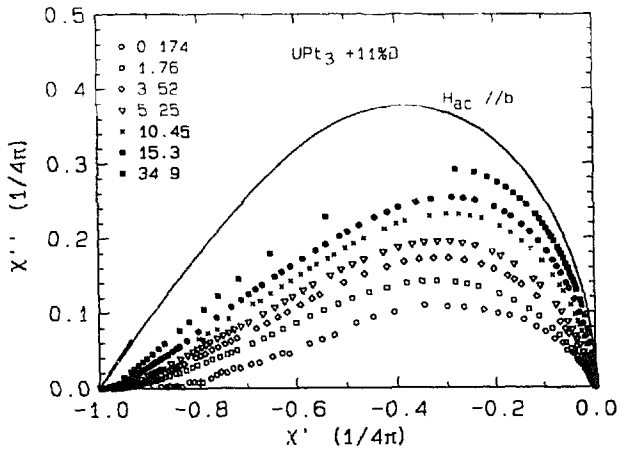

Fig. 5. The χ'' versus χ' plots obtained for a boron-doped sample (sample D) for the AC field parallel to the b-axis. Each set of data represents essentially the same results as those presented in fig. 2 but the temperature is used here as an implicit parameter. The AC field amplitudes (in Oe) are given in the figure. The solid curve is calculated using eq. (3–5), with $\lambda \to \infty$.

calculated using eqs. (3) and (5), in which $\lambda \to \infty$ has been assumed but δ has been used as a variable parameter. This corresponds to the situation of the normal state skin-effect susceptibility, or to the flux-flow regime where the same expression for χ is obtained as in the normal state, but the physical meaning of δ is different [33]. The convergence of the experimental curves towards the calculated one suggests that the large dissipation is due to the fact that the current density induced in the sample is higher than j_c. If that is the case, for any given temperature there should exist a region of AC field, where the crossover from the reversible (field independent susceptibility) to the critical state and then, with increasing field, to the flux-flow-like behaviour can be observed. The $\chi'' H_{AC}^2$ product (total loss signal) can be fitted within Campbell's model: above a certain AC field $H_0(T)$ the induced current density reaches the maximal possible value and then the losses become proportional to $(H_{AC}-H_0)^3$. However, this analysis must be treated as a first approximation. We can expect for instance a nonlinear current–voltage dependence, as it is observed in the vortex-glass state [34]. It would be useful to have a detailed model describing the response of a superconductor on the AC field in the case of nonlinear current–voltage dependence. At lower temperatures, when the imaginary part of the susceptibility is small, the AC field penetration depth λ can be calculated from the measurements of $\chi'(T)$. To do this, results similar to those in fig. 3 have been used together with eq. (5) for the AC susceptibility, in which the temperature independent, normal state δ is assumed (we verified that the choise of δ has small influence on this analysis). The outcome is presented in fig. 6 for the case without external DC field and for a few values of the DC field applied parallel to the AC field. Suprisingly, the results for $\lambda(T)$ cannot be fitted by the usual $\lambda = \lambda_0 (T_c - T)^{-\beta}$, with $\beta = \frac{1}{2}$; an exponent close to 1 is obtained, not $\frac{1}{2}$. The best fit is obtained with $\beta = 5/4$, though deviations are observed very close to T_c. If one ignores these deviations and determines T_c by extrapolating to $\lambda^{-4/5} = 0$ (the solid lines in fig. 6), T_c is found to depend on the applied DC field. This reflects the $H_{c2}(T)$ dependence, as we checked for higher fields with a better accuracy. The slopes of the solid lines in fig. 6 give λ_0 for various values of H_{DC}. As illustrated in fig. 7, the results are consistent with $\lambda_0(H_{DC}) = \lambda_0(0) + \gamma H_{DC}^{1/2}$. If we take for the characteristic dimensions of the c-axis and b-axis samples $d = 0.15$ and $d = 0.45$ mm, respectively, then the same values of λ_0 and γ are obtained for both field directions, within the accuracy of the measurements. The only results known to us giving a $\lambda(T)$ dependence with the exponent β close to 1, are the high-field measurements on high-T_c materials [35] in the temperature range where vortices are strongly pinned to the lattice. Due to the small external AC field they

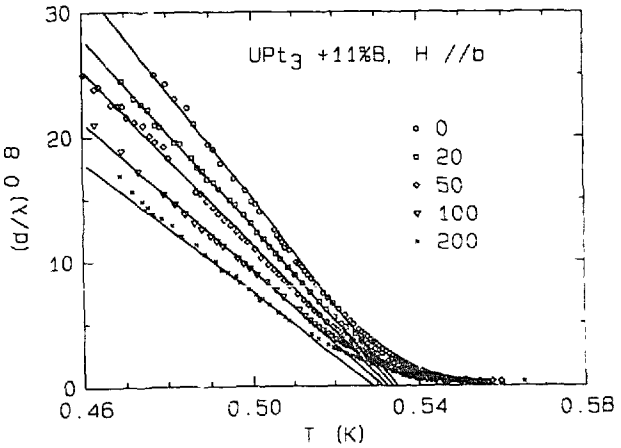

Fig. 6. $(d/\lambda)^{0.8}$ as a function of temperature for different DC fields, determined from the data of fig. 3, for field parallel to the b-axis of the sample doped with boron.

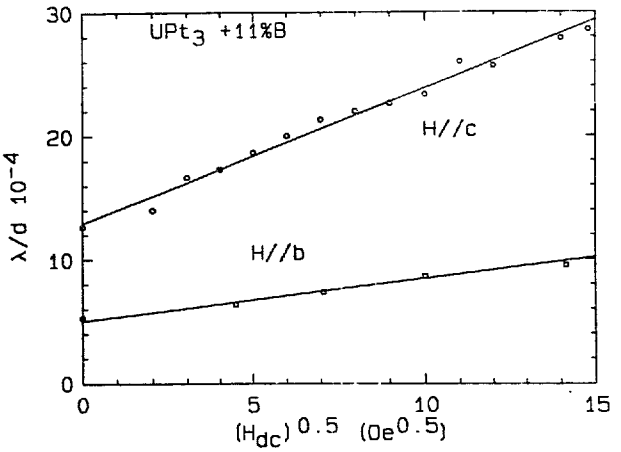

Fig. 7. λ_0/d as a function of $H_{DC}^{1/2}$ for boron-doped samples. The lower curve is obtained for field parallel to the *b*-axis and the upper one for field parallel to the *c*-axis. Note that the sample dimension *d* is different for both samples (cf. table 2).

oscillate in their potential minima giving a contribution to the reactive component of the impedance. In order to describe the properties of such a system, we need a relation between the electric field and the supercurrent density. This problem has been treated lately in a few publications, for instance by Coffey and Clem [36]. Generally, the normal-state skin depth δ, the skin depth arising from the vortex motion, the London penetration depth λ_L, and the Campbell penetration depth λ_p enter into the formula for the complex impedance of the superconductor. In our case it should be sufficient to take into account the Campbell penetration depth, only. We find then that the desired relation between the supercurrent and electric field is similar to the London equation, the only difference being that the London penetration depth λ_L is replaced by λ_p, given by ref. [36] (in the limit $\lambda_p \gg \lambda_L$):

$$\lambda_p^2 = \frac{B\Phi_0}{4\pi k} . \tag{7}$$

Above, the Labusch parameter k is connected with the curvature of the pinning potential. The precise form of $k(T)$ is not known and it depends on the details of the pinning mechanism. However, at low fields, k should be proportional to the condensation energy per unit length of a single vortex line,

$$k(T) = pH_c(T)^2/\kappa_{GL}^2 , \tag{8}$$

where κ_{GL} is the Ginzburg–Landau parameter and p some constant, usually assumed to be between 10 and 10^2, due to vortex interaction. The temperature dependence of $k(T)$ which follows from eq. (8), is observed in experiments on high-T_c materials [37]. The temperature dependence of the penetration depth λ_p which follows eqs. (7) and (8), with the exponent β close to 1, is in agreement with our results for the penetration depth measured in the superimposed DC field. We see that eq. (7) gives the desired field dependence, in accordance with our observations as well (fig. 7): $\lambda_p \sim B^{1/2}$. The very approximately calculated amplitude of this effect, with $H_c(0) = 250$ Oe and κ_{GL} about 30 is in agreement with the observed slope $d\lambda_p/dH_{DC}^{1/2}$ in fig. 7, if the parameter $p \approx 10^2$ is used. A problem arises with the interpretation of the temperature dependence of the penetration depth without applied DC field, as it has the same form as in the case with the applied field. The latter could be understood if the presence of vortices in the bulk superconductor in zero external field is assumed. (We do not think that the penetration of the AC field of a small amplitude may create the number of vortices sufficient to explain the results; moreover, χ' and consequently the penetration depth are practically independent of AC field amplitude at very small AC field amplitudes.) However, vortices may be present in zero external field in the case of UPt_3 where an interaction exists between the AF and unconventional SC order parameters, which may lead to the formation of the vortex-glass state even without external field, as argued by Joynt et al. [29]. An important aspect of the results reported here is the possible connection with earlier attempts to determine H_{c1} and its temperature dependence. We have argued that the procedure of $\chi'(H_{DC})$ measurements is not suitable to obtain H_{c1}. In fig. 8 the H–T phase diagrams constructed from the $\chi(T)$ measurements for different H_{AC} amplitudes are shown. The data represent the temperature points, below which χ'' becomes temperature independent (and equal to zero, within the experimental accuracy) for a given AC field. This method is used sometimes to determine $H_{c1}(T)$ [38]. For comparison, fig. 8 also contains the data for the first critical field measured on the same samples [26] by the DC method. Both sets of curves should be discusses in terms of the critical current density rather then connecting them with

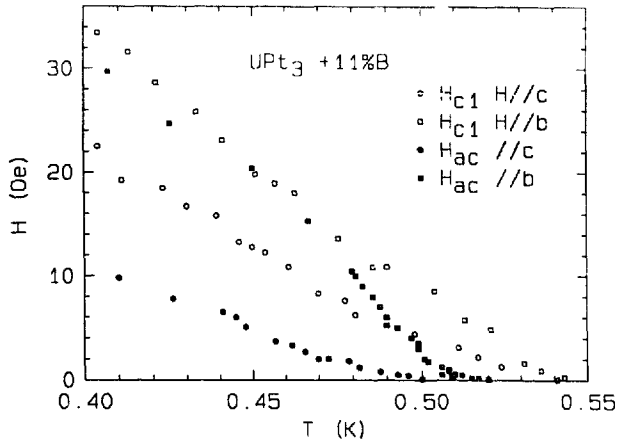

Fig. 8. Temperatures and AC field amplitudes where the offset of $\chi''(T)$ is observed, determined form the data similar to those in fig. 2, (filled symbols), compared with the first critical field results for the same samples, taken from ref. [26], (open symbols). The squares are for the AC or DC field parallel to the *b*-axis and the circles for field parallel to the *c*-axis.

$H_{c1}(T)$, despite the coincidence of the data for sample D at lower temperatures (close to T_c there is no such agreement). The field values of fig. 8 are close in order of magnitude to the thermodynamic critical field, no to H_{c1}, as noted by Vincent et al. [22] in connection with attempts to determine H_{c1} from $M(T)$ measurements. As noted earlier, the strong amplitude dependence of the AC susceptibility might be discussed in terms of a nonlinear current–voltage dependence. The temperature dependence of δ has been neglected by us, while in the superconducting state the real component of the complex conductivity (to which δ is related) should change strongly close to T_c. These problems will be addressed in further investigations. Another approach to the above results and to an interpretation of the low field electrodynamic properties of UPt_3 would be to consider the possible role of the formation of a surface energy barrier for flux entrance into the sample, the phenomena discussed by Bean and Livingston [39]. There are some results of Pollini [19] giving evidence for the existence of such an energy barrier and some of our results could be understood in these terms. However, this is a difficult experimental problem, requiring a large number of further investigations.

5. Conclusion

A large anisotropy of the AC susceptibility for a field directed along the *b*- and *c*-axes of single-crystalline samples of pure and boron-doped UPt_3 is observed. The double-step superconducting transition in $C(T)$ is also visible in $\chi(T)$ for the pure UPt_3 sample measured with fields parallel to the *c*-axis, but some features of the double-step transition can be found from the detailed analysis of results for all samples. The penetration depth close to T_c cannot be described by the conventional dependence with the critical exponent β equal to $\frac{1}{2}$; instead, we find β close to 1. The results are qualitatively consistent with the assumption of the existence of a spontaneous vortex state in the sample. An interaction between current and trapped vortices modifies the effective penetration depth and its temperature dependence. The possible origin of vortices in the absence of an external field is the formation of the vortex-glass state due to the interaction between the unconventional SC order parameter and antiferromagnetism. At a given temperature, for a low AC field the response of the samples is linear as a function of field amplitude. This is explained by assuming that the supercurrent induced in the material has smaller value than the critical supercurrent density [27,28], not as a signature of the Meissner state. It is argued that earlier measurements of $H_{c1}(T)$ from DC magnetization, performed also on two of our samples, are not really giving the first critical field values but should be discussed in terms of the critical current density. The above effects are sample dependent and one should keep in mind that they may be caused by inhomogeneities. However, the large temperature interval in which they are observed and the high values of T_c of our samples, with a well-developed two-step transition in $C(T)$, expecially for samples doped with boron, make this very unlikely.

Acknowledgement

ZK is gratefull to M. Sigrist and C.J. van der Beek for helpful remarks touching the content of this work.

References

[1] M. Sigrist and K. Ueda, Rev. Mod. Phys. 63 (1991) 239.
[2] B.S. Shivaram, Y.H. Yeong, T.F. Rosenbaum and D.G. Hinks, Phys. Rev. Lett. 56 (1986) 1078.
[3] A. Schenstrom, M-F. Xu, Y. Hong, D. Bein, M. Levy, B.K. Sarma, S. Adenwalla, Z. Zhao, T. Tokuyasu, D.W. Hess, J.B. Keterson, J.A. Sauls and D.G. Hinks, Phys. Rev. Lett. 62 (1989) 332.
[4] A. de Visser, A.A. Menovsky, J.J.M. Franse, K. Hasselbach, A. Lacerda, L. Taillefer, P. Haen and J. Flouquet, Phys. Rev. B 41 (1990) 7304.
[5] K. Hasselbach, A. Lacerda, K. Behnia, L. Taillefer, J. Flouguet and A. de Visser, J. Low Temp. Phys. 81 (1990) 299.
[6] B.S. Shivaram, J.J. Gannon Jr. and D.G. Hinks, Physica B 163 (1990) 141.
[7] K. Behnia, L. Taillefer, J. Flouquet, D. Jaccard, K. Maki and Z. Fisk, J. Low Temp. Phys. 84 (1991) 261.
[8] B.S. Shivaram, J.J. Gannon Jr. and D.G. Hinks, Physica B 163 (1990) 629.
[9] L. Taillefer, Physica B 163 (1990) 278.
[10] C.H. Choi and J.A. Sauls, Phys. Rev. Lett. 66 (1991) 484.
[11] R.A. Fisher, S. Kim, B.F. Woodfield, N.E. Philips, L. Taillefer, K. Hasselbach, J. Flouquet, A.L. Giorgi and J.L. Smith, Phys. Rev. Lett. 62 (1989) 1411.
[12] D.W. Hess, T.A. Tokuyasu and J.A. Sauls, J. Phys.: Condens. Matt. 1 (1989) 8135.
[13] R. Joynt, Supercond. Sci. Technol. 1 (1988) 210.
[14] K. Machida and M. Ozaki, J. Phys. Soc. Jpn. 58 (1989) 2244.
[15] F. Gross-Alltag, B.S. Chandrasekhar, D. Einzel, P.J. Hirschfeld and K. Andres, Z. Phys. B 82 (1991) 243.
[16] J.J. Gannon Jr., B.S. Shivaram and D.G. Hinks, Europhys. Lett. 13 (1990) 459.
[17] W.O. Putikka, P.J. Hirschfeld and P. Wolfle, Phys. Rev. B 41 (1990) 7285.
[18] A. Pollini, A.C. Mota, P. Visani, G. Juri and J.J.M. Franse, Physica B 165–166 (1990) 365.
[19] A. Pollini, Ph.D. Thesis, ETH Zurich (1991).
[20] Y.Yeshurun, A.P. Malozemoff, F. Holtzberg and T.R. Dinger, Phys. Rev. B 38 (1988) 11828.
[21] C. Broholm, G. Aeppli, R.N. Kleiman, D.R. Harshman, D.J. Bishop, E. Bucher, D.L. Williams, E.J. Ansaldo and R.H. Heffner, Phys. Rev. Lett. 65 (1990) 2062.
[22] E. Vincent, J. Hammann, L. Taillefer, K. Behnia, N. Keller and J. Flouquet, J. Phys.: Condens. Matt. 3 (1991) 3517.
[23] F. Piquemal, J. Flouquet, J.L. Tholence, J.J.M. Franse and A. Menovsky, J. Magn. Magn. Mater. 63&64 (1987) 469.
[24] Z. Koziol, K. Bakker, A. de Visser and J.J.M. Franse, Proc. M^2S-III Conf., Kanazawa, Physica C 185–189 (1991) 2633.
[25] T. Vorenkamp, A. de Visser, R. Wester, A.A. Menovsky and J.J.M. Franse, Physica B 165–166 (1990) 363.
[26] E.A. Knetsch, J.A. Mydosh, T. Vorenkamp and A.A. Menovsky, preprint, ICM, Edinburgh, 1991.
[27] A.M. Campbell, J. Phys. C 4 (1971) 3186.
[28] A.M. Campbell, J. Phys. C 2 (1969) 1492.
[29] R. Joynt, V.P. Mineev, G.E. Volovik and M.E. Zhitomirsky, Phys. Rev. B 42 (1990) 2014.
[30] A.A. Menovsky and J.J.M. Franse, J. Crystal Growth 65 (1983) 286.
[31] L.D. Landau, E.M. Lifshitz, Electrodynamics of Continuous Media (Pergamon, New York, 1960) p.193.
[32] C.P. Bean, Rev. Mod. Phys. 36 (1964) 31.
[33] V.B. Geshkenbein, V.M. Vinokur and R. Fahrenbacher, Phys. Rev. B 43 (1991) 3748.
[34] D.S. Fisher, M.P.A. Fisher and D.A. Huse, Phys. Rev. B 43 (1991) 130.
[35] A.F. Hebard, P.L. Gammel, C.E. Rice and A.F. Levi, Phys. Rev. B 40 (1989) 5243.
[36] M.W. Coffey and J.R. Clem, Phys. Rev. Lett. 67 (1991) 386.
[37] Dong-Ho Wu and S. Sridhar, Phys. Rev. Lett. 65 (1990) 2074.
[38] Y. Yamaguchi, M. Tokumoto and K. Mitsugi, Physica C 179 (1991) 447.
[39] C.P. Bean and J.D. Livingston, Phys. Rev. Lett. 12 (1964) 14.
[40] Z. Zhao, F. Behroozi, Y. Guan, J.B. Ketterson, B.K. Sarma and D.G. Hinks, Physica B 165–166 (1990) 345.